

# Determination of instability of the fault zone model

G. A. Sobolev and A. V. Ponomarev

Institute of Physics of the Earth, Russian Academy of Sciences, Moscow

**Abstract.** A series of experiments was carried out with three-layer models constructed of granite chippings, quartz sand, and cement; the inner layer of the models had lower strength. The models were loaded on a servocontrolled press under biaxial compression and supplementary mechanical vibration with 40 and 120-sec periods. The variations in press rigidity allowed both to obtain friable macrodestruction of the inner layer and to conduct the experiment in the post-peak stress state with accumulation of microdestruction. Stress, deformation, and acoustic emission were recorded in the course of the experiment, and ultrasonic sounding was also periodically employed. The main object of research was to find symptoms of transition of the model into the stage of unstable deformation in the absence of the rheological curve. We have established that this transition can be revealed by several indicators, i.e., the appearance of asymmetry in the compression-extension phases of vibration cycles, accumulation of diversity of deformations recorded by spatially distributed sensors, distortion of the waveform during ultrasonic sounding, the growth of the “seasonal” amplitude of the acoustic emission showing an increase in the strain sensitivity of the medium, the appearance of the acoustic silence and subsequent activation. We presume that these symptoms can be used to estimate the onset of the instability stage in the fault zones of the Earth’s crust when analyzing the weak seismicity, Earth tides and vibroseis data.

## Introduction

One of the main problems in earthquake source physics and earthquake prediction is the problem to reveal the stage of rock instability in the Earth’s interior. The mechanics of solid bodies and rock failure strongly imply, in particular, that the macrodestruction of a loaded body occurs at the so-called post-peak stage of deformation, when the load reaches its ultimate value and begins to decline as the deformation accelerates. At this stage, the loaded body releases the accumulated elastic energy. In the laboratory, this stage is easily enough determined, since there is a possibility to record the rheological stress-deformation curve. A complex of laboratory and field researches shows [Sobolev, 1993; Sobolev and Kol’tzov, 1988] that, at the post-peak stage of deformation, various precursors of a future macrorupture appear, the dynamic spreading of which causes an earthquake.

In the nature environment of a seismically prone area it is impossible for the researcher to measure the stresses and deformations in the Earth’s deep interior, where the earthquake sources actually develop. The discovery of the means for instability state determination from indirect technique should, therefore, greatly improve the earthquake prediction research. The Earth is subjected to the mechanical effects of earth tides with their highest values in the semidiurnal, diurnal, fortnightly and monthly periods. Although numerous attempts were made to use earth tides for evaluation of seismic hazards [Mikumo *et al.*, 1978; Nikolaev and Nikolaev, 1993; Nishimura, 1950; Xiang-chu Yin *et al.*, 1994] the problem is still well beyond solution.

One of the reasons is the inadequate knowledge of the mechanism of the effect of mechanical vibrations on the development of the instability process in geologic environment. The influence of vibrations, used as an additional effect to the main load, may change the destruction process itself. In [Sadovsky *et al.*, 1981; Sobolev and Ponomarev, 1996] the authors show that this kind of influence on the samples of different rocks and man-made materials encourages transition from brittle destruction to the release of elastic energy, accumulated by the sample, through plastic deformation. It was es-

---

©1999 Russian Journal of Earth Sciences.

Paper No. TJE99016.

Online version of this paper was published on July 20 1998.  
URL: <http://eos.wdcb.rssi.ru/tjes/TJE99016/TJE99016.htm>

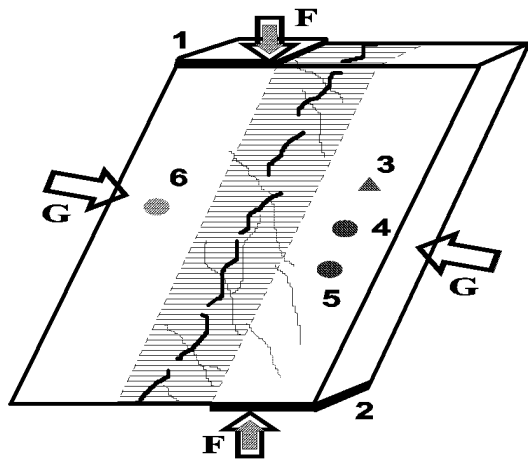


**Figure 1.** The scheme of the model: 1, 2 – tensometers; 3 – acoustic emission receiver; 4, 5, 6 – emitter and receivers of elastic impulses for ultrasonic sounding.

tablished [Sobolev *et al.*, 1996], that additional vibration results in shorter time intervals between consecutive movements of the stick-slip type on the contact between blocks of rock. The influence of some other factors on development of instability in rocks was investigated by Sammonds *et al.* [1992].

The purpose of this paper is to find a set of indicators that can help discover the transition of the simple fault zone model to the instability stage without knowledge of the absolute values of applied stresses and deformations. We suggest that this approach can be realised in natural environment to determine the stages of the earthquake source development.

## Methods

The experiments were carried out on models built of granite chips of different size ranging from 2 to 20 mm, quartz sand, and concrete. Figure 1 shows the general view of the model. The two lateral layers were stronger than the central layer owing to the 400-brand cement that was used to make them, whereas the 50-brand cement was the binding component in the central layer. The initial average velocities of compressional waves in the lateral layers were 4 km/s and in the central layer 3 km/s. The length of the model on its side facet was 300 mm, the width along the perpendicular was 220 mm. The size of the model in its third dimension was 65 mm. The thickness of the lateral and central layers was the same. Owing to the jutting out corners of the chips, the contacts between the lateral and central layers were rough, and the average angle of their dip towards the vertical axis coincided with the main

load  $F$  and was 25. The lateral compression stress  $G$  was 4 tons and was maintained constant throughout the experiment with the accuracy of 1% by roller padding between the side facets of the model and the pistons of the press. The vertical load  $F$ , also applied by roller padding, was gradually increased to its peak value and then reduced in the post-peak area of deformation to correspond to the condition of the constant strain rate  $\varepsilon = 0.5 \cdot 10^{-6}$ .

The experiments were conducted on the “Inova” press, with a servocontrol, at the Borok Observatory of the Institute of Physics of the Earth. The load  $F$  and the movement of the pistons in the vertical direction  $D$  were recorded with sampling rate of 1 s on PC IBM. The present paper is based on the results of 13 experiments seven of, which had load  $F$  modulated, by additional vibration with 40 s periods and the rest with 100 s periods. The amplitude of vibration was about 12% of load  $F$ . The choice of construction of the models and the type of loading has caused formation of cracks and their development in the weaker central layer. A system of echelonlike fractures appeared, the typical case of which is shown in Figure 1. The macrodestruction occurred as a rupture of the shear type cutting across the system of echelonlike fissures along the central layer. Besides the measurement of stress applied to the model recorded by the “Inova” press system, the calibrated stress testers 1 and 2 were mounted on two sides of the model between its upper and lower facets and the pistons of the press. The testers were steel prisms with glued-on strain gauges operating in the linear regime; their  $F$  values were recorded on PC every second.

The acoustic signals that appeared during the deformation were recorded on PC-IBM by a 3-channel system composed of acoustic emission (AE) receivers, amplifiers with analogue filters (the lower range of the pass band is 30 kHz), discriminators of the AE signals, and digital recorders with a storage modulus. The TS-19 piezoceramic discs were used as the sensitive element on the AE receivers. The three-channel scheme divided the AE signals into three paths with different minimal amplitude levels of discrimination in 1:2:4 ratios. Concurrently, the level of the first channel was tuned to receive AE signals with amplitudes twice as large as that of noise. The storage recorder accumulated AE signals during 1 s time period and then transferred the digital information on acoustic activity to the memorising device.

In the course of the experiment usually lasting several hours, the model was periodically sounded to measure the elastic waveforms and velocities in two directions: 4–5 and 4–6 (Figure 1). The frequency spectrum of the longitudinal wave impulse passing through the model was in the range of tens of kHz. The sounding was carried out at the moments of maximum and minimum vibration amplitude.

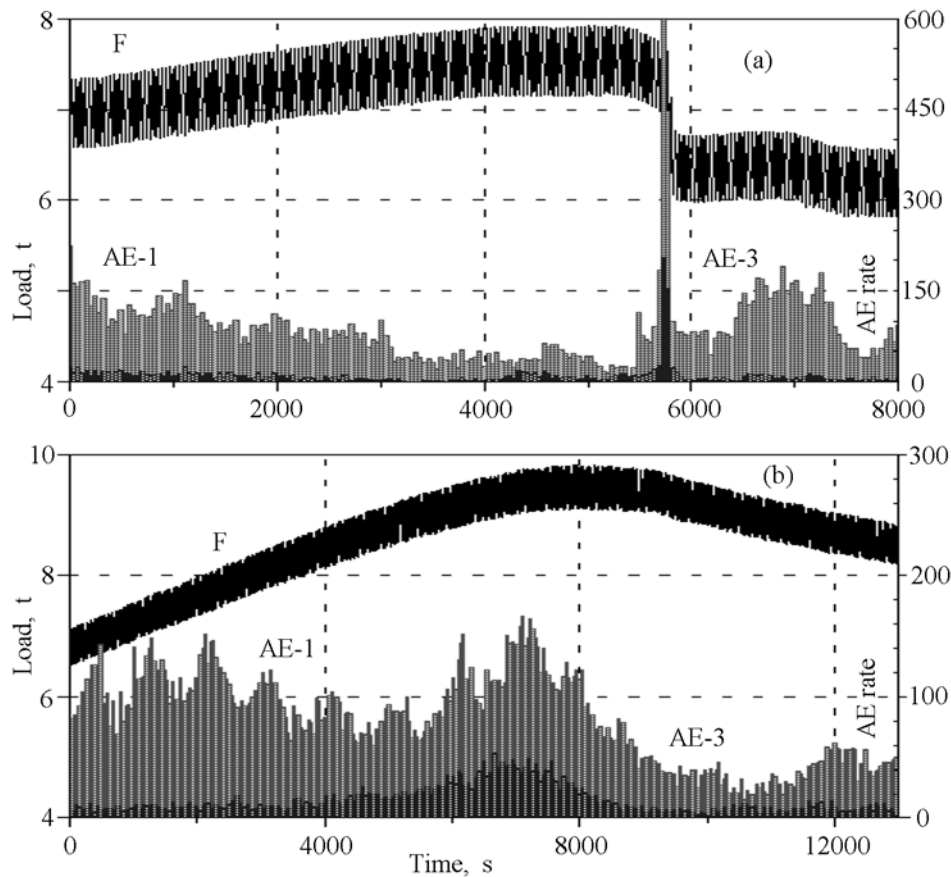


**Figure 2.** Examples of variations of  $F$  load and acoustic emission (number of signals per 1 s) on channels with different sensitivity in the experiment with a supplementary spring No.11 (a) and without it No. 13 (b).

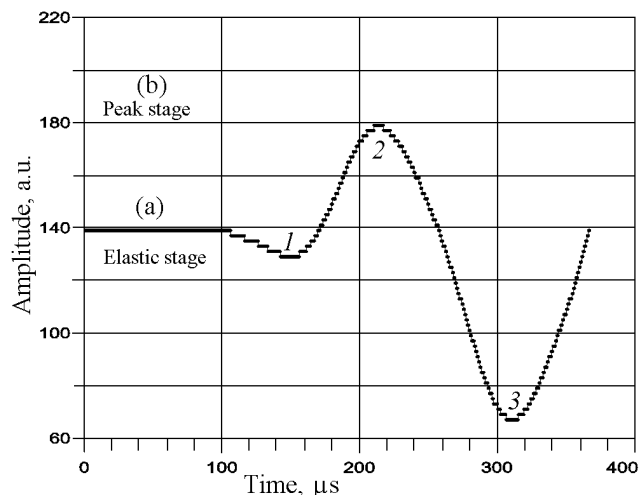
## Results

Figure 2a,b shows the curves of load  $F$  in two typical experiments No.11 and No.13, which demonstrate only the last stages of the experiment, when  $F$  values have reached about 50% of their maximal value. The first stage of elastic behaviour of the model is not significant for the purpose of this study. In this pattern of research, the experiments such as No.11 (Figure 2a) differed from those, which were analogous to No.13 (Figure 2b), in that, in the first case, there were springs installed between the pistons of the press and the facets of the model. This instalment resulted in lesser rigidity of the loading system and caused the dynamic development of a macrorupture in the post-peak stage of deformation followed by a sudden release of load  $F$ . In both cases on Figure 2 the plots of the common strain of the model grew linearly in the course of the experiment.

The lower part of Figure 2 shows the plots of acoustic emission on two channels: the most sensitive AE1 and the least sensitive AE3. In both types of experi-

ments they show the same characteristics. At the non-elastic stage of deformation, the periods of acoustic quiescence are followed by the stage of activation. Its maximum in the experiments without the supplementary spring (Figure 2b) commenced somewhat earlier than the maximum of load  $F$ . In the experiments with the supplementary spring, this maximum, naturally, coincided with the moment of dynamic macrorupture development accompanied by load release. The acoustic quiescence is manifested on the channel that recorded weak events of AE1. On the contrary, the number of signals of relatively high amplitude slowly grows towards the maximum of loading (AE3 channel). A similar peculiarity was already noted earlier in the course of modelling the situation in the “seismic gap” [Salov *et al.*, 1987]. We adhere to the following explanation of this fact: the formation of relatively large fracture causes unloading of the material between them and creates unfavourable conditions for development of smaller cracks in the bulk of the deformed body.

The main purpose of these experiments was to de-



**Figure 3.** An example of the change in ultrasonic impulse form in experiment No. 11: (a) – the elastic stage of loading, (b) – the stage of maximum  $F$  load. 1,2,3 – characteristic impulse points applied for the analysis of kinematic and dynamic characteristics.

termine whether we can establish the transition to the stage of instability and recognise the macrorupture precursors without knowing the outer load  $F$  and the common strain of the model. We shall further set forth consecutively the results of analysis of different indicators.

The periodic sounding of the model in the kHz frequency band made it possible to observe the changes in the running times and wave forms of impulses. Figure 3 shows, as an example, the forms of the first phase of longitudinal waves at the elastic stage of deformation (Figure 3a) and at the load  $F$  maximum (Figure 3b) in the No.11 experiment. The periods of the phases of the 1-st minimum  $t_1$ , of the maximum  $t_2$ , and of the 2-nd minimum  $t_3$  gradually increased in the course of the experiment, which fact corresponded to the decrease in wave velocity. The increase of periods, however, was not proportionate, which caused distortion of the signal. A comparison of Figures 3a and 3b revealed that, with the general increase of the visible period of the impulse ( $t_3 - t_1$ ) from 16 mcs to 17.5 mcs, the time of the maximum shifted by 2.6 mcs, whereas the time of the second minimum shifted only by 1.5 mcs. This process is accompanied by a considerable reduction of the amplitude of  $A_{21}$  signal between maximum 2 and minimum 1, if compared with the reduction of the amplitude of the next  $A_{23}$  phase. Accordingly, the  $A_{23}/A_{21}$  ratios grew, as demonstrated by the run of these plots in Figures 4-5.

In order to estimate the changes only in the form of ultrasonic impulses passing through the model, they were reduced to one and the same amplitude  $A_{23}$ . After that, the areas of the first and second parts of the impulse were calculated, i.e.,  $S_{12}$  and  $S_{23}$ . It was established that the  $S_{23}$  area gradually grew following the elongation of the second part of the impulse from  $t_2$  to  $t_3$  time. Concurrently, a corresponding elongation of the first part of the impulse from  $t_1$  to  $t_2$  did not compensate the reduction of amplitude  $A_{12}$  and, therefore, the  $S_{12}$  area decreased as a consequence, their  $S_{23}/S_{12}$  ratio grew.

The loading pattern was constructed so that the span of amplitudes in the consecutive vibration cycles changed in proportion to the applied load  $F$ . It seemed natural to assume that, with the same reaction of the model to the phases of relative compression and tension in vibration cycles, the amplitudes of phases of compression  $A_c$  and tension  $A_t$  shall change in proportion to one another, and their  $A_t/A_c$  ratio shall approach a constant value. This did not happen, however. Figure 4 shows the graphs of  $A_t$ ,  $A_c$ , and  $A_t/A_c$  in the No.11 experiment. Only a part of the experiment is shown here up to the moment of macrorupture (see Figure 2a). For the sake of convenience, load  $F$  is represented by an averaged curve without the periodic vibration. An analysis of the  $A_t$  and  $A_c$  amplitudes shows that, from the time of about 3000 seconds, the amplitude of the compression phase  $A_c$  regularly decreased. This period corresponds to a bend in the load  $F$  curve, which indicates transition of the model to the stage of non-elastic deformation. The amplitude of the

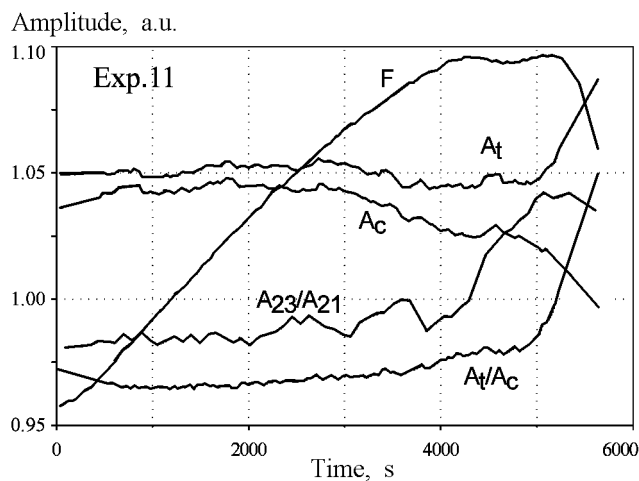


**Рис. 4.** Variations of  $F$  load (without vibration); ratios of vibration amplitudes in  $A_c$  compression and  $A_t$  tension phase, their  $A_t/A_c$  relations, and also relations of  $A_{23}/A_{12}$  amplitudes in the impulse during ultrasonic sounding in the experiment with supplementary spring No.11. The period of vibrations is 40 s.

tension phase  $A_t$  in this interval remained on an approximately constant level. Consequently, the  $A_t/A_c$  ratio slowly grows. A rapid growth of  $A_t$  and further decrease of  $A_c$  mark the stage of deformation instability before the macrorupture. This symptom is indicated by a sudden increase of  $A_t/A_c$ , and can be assumed as a precursor of macrorupture.

In experiment No.11, the period of supplementary vibration was 40 s. The same peculiarities in  $A_t/A_c$  behaviour were also recorded in the experiments with the 120-s vibration period. For example, Figure 5 shows the result of experiment No.10, which was also carried out with a supplementary spring. The right-hand part of the figure is limited by the moment of dynamic macrorupture that caused  $F$  release. The  $A_t/A_c$  ratio slowly grows during the non-elastic stage of deformation and suddenly accelerates in the post-peak stage. The occurrence of a precursor of macrorupture is obvious.

Let us now analyse the behaviour of this parameter in the experiments without the supplementary spring, when the high-speed feedback of the “Inova” press prevented the dynamic propagation of macrorupture. The latter occurred as a result of gradual accumulation of microdefects, while the experiment itself continued in the post-peak stage of deformation without loss of the bearing capacity of the model. An analysis of typical experiments shows that there is a bend in the  $A_t/A_c$  course, while the amplitude of compression phase attenuated more quickly. As a result, the  $A_t/A_c$  grows. This increase of the vibration cycle asymmetry is continued in the post-peak deformation area, and then it stabilises. This process differs from the discussed above examples shown in Figures 4 and 5 by the absence of a sudden growth of  $A_t/A_c$  at the start of the post-peak stage of deformation.

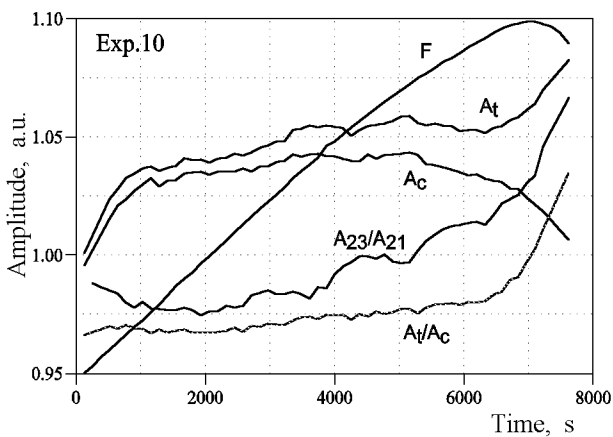


**Fig. 5.** Ditto as in Figure 4, in the experiment with the supplementary spring No. 10. The period of vibration is 120 s.

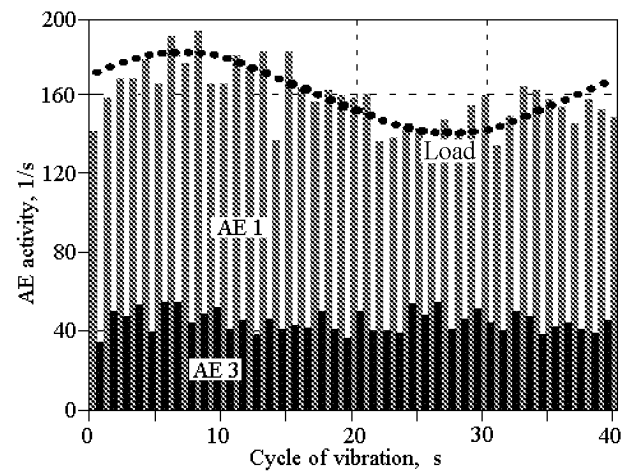


**Figure 6.** An example of acoustic emission variations along channels of high AE 1 and low AE 3 sensitivity as compared with the sinusoidal period of vibration.

Since the vibration period was rigorously conditioned by the generator and remained unchanged during the course of each experiment, the asymmetry in the amplitudes of the compression and tension phases resulted in the corresponding asymmetry of the areas of half-cycles of compression-tension, and their ratio changed similarly to  $A_t/A_c$ . In Figures 4–5, the demonstrated behaviour of  $A_t/A_c$  parameter and that of  $A_t$  and  $A_c$  amplitudes separately did not qualitatively change in the course of the analysis of data recorded by the stress testers installed at the upper and lower facets of the model. The difference between the data of the testers was also analysed: it slightly grew with the progress of the experiment and reached its highest value not in the period of the maximal load  $F$ , but with a certain delay, which evidently reflected the process of cracks accumulation. Special calibration tests, carried out on steel plates and cylinders, have shown identical operation of stress testers used in the experiment.

A “seasonal pattern” of the acoustic emission was observed during the consecutive vibration cycles of compression-tension. It is shown in comparison with the sinusoidal curve of one vibration cycle on Figure 6. During the compression phase, the number of acoustic signals in a time unit increased, and during the tension phase their number was reduced.

## Discussion of results

The discovered effect of asymmetry in the development of the initially sinusoidal vibration cycles (plots  $A_t/A_c$  in Figures 4–5), as we think, is indicated by the following symptoms. The pistons create additional vibration because the generator of sinusoidal signals sup-

plies the sign-variable voltage to the servovalve. During the elastic stage of experiment, the deformation modulus in the loading stage ( $+dF/dD$ ) is approximately equal, with a reversed sign, to the elasticity modulus in the unloading stage ( $-dF/dD$ ), and the  $dF/dD$  oscillations occur along one and the same almost straight rheological curve; correspondingly, the mechanical stresses developed by the press and recorded by testers 1 and 2 are equal. At the nonelastic stage the model becomes softer owing to the microcracking process. Consequently, during the loading stage, the press cannot develop the stress corresponding to the voltage supplied to the servovalves. During unloading the rheological curve becomes steeper.

At the post-peak (unstable) stage before the macro-rupture, the model releases the elastic energy accumulated earlier. This phenomenon, in the nonabsolute rigidity conditions of the loading system, causes the growth of  $A_t$  amplitude in the phase of relative tension. This effect is enhanced during the unstable macro-rupture development ( $A_t/A_c$  plots in Figures 4 and 5).

The superficial similarity of behaviour of ultrasonic impulses parameters during sounding is attributed to another mechanism, i.e., the growth of  $A_{23}/A_{21}$  ratio occurs not as a result of the predominant growth of  $A_{23}$  amplitude, but owing to a sharper decrease of  $A_{12}$ . We suggest that this effect be caused by considerable attenuation of high frequencies, which are energybearing in the first part of the ultrasonic impulse. This is also testified by the predominant reduction of the area of the first part of the impulse. The accomplished calculations show that the frequency spectra of impulses shift to the low-frequency area as the deformation of the model progresses, and the corresponding shifts are observed in the components of periodograms. As the cracks accumulate, the distortion of the spectral composition, by the way, is not unexpected. It is only important that this effect is reliably recorded and that it appears in a set of dynamic characteristics of the signals.

It should be noted that the "seasonal pattern" of the acoustic emission appeared only on the highly sensitive AE1 channel, i.e., during the registration of relatively weak acoustic events. The following preliminary explanation is suggested. It is common knowledge that from the point of view of kinetics conception of durability, the formation of fractures begins after a certain time period as soon as the load reaches the durability limit. Destruction is a time dependent process. It is quite probable that the formation of a large fracture requires a longer time lag. In this case, the appearance of relatively strong acoustic signals is shifted, in relation to the sinusoidal  $F$  vibration cycles, to unknown to us and different time intervals, and we do not find significant correlation between the number of acoustic signals and  $F$  value.

## Conclusions

The main inference of the accomplished research is as follows. It was determined that by creating oscillations in the deformed body and by studying the changes in their dynamic characteristics we can fix the onset of the stage of mechanical instability of the body and reveal precursors of macrodestruction in the absence of data about the absolute values of the load applied to the body and about deformation. The principal prognostic feature is the distortion of form of the harmonic or impulse sounding signal. The effect is enhanced by the soft (padded) loading system, which promotes more brittle macrodestruction.

This approach, apparently, can be realised under the Earth's conditions when studying the reaction of the rock massif to earth tides or man-made signals of vibrosounding. These studies can be of practical importance for prediction of earthquakes and rock bursts by periodic sounding of potential earthquake source and rock blocks in mines. This method can be, perhaps, applied when estimating the stability of foundations of buildings and during the non-destructive control of constructions.

**Acknowledgements.** The authors are grateful for assistance in measurements to their colleagues at the United Institute of Physics of the Earth, RAS, – O. V. Babichev, A. V. Kol'tsov, A. O. Mostryukov, A. V. Patonin, B. G. Salov. This research was supported by the Russian Foundation for Basic Research, project No. 97-05-64485.

## References

- Mikumo, T., Rato M., Doi, H. et al., *Earthquake precursors*, pp. 123–136, Japan Scientific Societies Press, 1978.
- Nikolaev, A. V. and Nikolaev, V. A., Earth tides triggering of earthquakes, *Continental Earthquakes*, pp. 319–327, Seismological Press, Beijing, 1993.
- Nishimura, E., *On earth tides*, Trans. Am. Geophys. Union, 31: 357–376, 1950.
- Sadovsky, M. A., Mirzoev, K. M., Negmatullaev, S. Kh., and Salomov, N. G., The effect of mechanical vibration on the plastic deformation features of materials, *Izv. Acad. Sci. USSR, Phys. Earth*, (6), 32–42, 1981 (in Russian).
- Salov, B. G., Potuzak, Z., Irisova, E. L., and Sobolev, G. A., Acoustic emission precursors of shear fracture, *Acta Montana*, 75, 245–254, 1987.
- Sammonds, P. R., Meredith, P. G., and Main, I. G., Role of pore fluids in the generation of seismic precursors to shear fracture, *Nature*, 359, 228–230, 1992.
- Sobolev, G. A., *Basic principles of earthquake prediction*, Nauka, Moscow, 1993 (in Russian).
- Sobolev, G. A. and Kol'tsov, A. V., *Large-scale modelling of the preparation of earthquakes and of earthquakes precursors*, Nauka, Moscow, 1988 (in Russian).

- Sobolev, G. A. and Ponomarev, A. V., *The effect of harmonic oscillations on the deformation and acoustic regime of the fault zone model*, *Seismology in Europe*, pp. 94–99, European Seismological Commission, Reykjavik, 1996.
- Sobolev, G. A., Ponomarev, A. V., Koltzov, A. V., and Smirnov, V. B., Simulation of triggering earthquakes in the laboratory, *PAGEOPH*, 147, (2), 345–355, 1996.
- Xiang-chu, Yin, Xue-Zhong, Chen, Zhi-ping, Song and Can, Yin, The load-unload response ratio (LURR) theory and its application to earthquake prediction, *Journal of Earthquake Prediction Research*, 3, (3), 325–333, 1994.

(Received March 15, 1999.)

## Определение стадии неустойчивости модели разломной зоны

Г. А. Соболев, А. В. Пономарев

### Аннотация

Выполнены эксперименты на моделях геологической среды в условиях двухосного сжатия с дополнительной осевой синусоидальной нагрузкой. Модели состояли из двух внешних слоев повышенной прочности и центрального слоя пониженной прочности, который включал щебень различного размера. Конструкция моделей и выбранный режим нагружения позволяли реализовать классический тип разрушения с накоплением субпараллельных кулисообразных

трещин во внутреннем слое и последующим сдвиговым макроразрывом. Эксперименты выполнялись при средней скорости продольной деформации  $0.5 \times 10^{-6} \text{ с}^{-1}$ . Период силовой вибрации с амплитудой около 12% от текущей нагрузки составлял 40 или 120 с. В процессе нагружения регистрировались изменения нагрузки с помощью двух датчиков напряжений на верхней и нижней гранях модели, а также волновые формы при периодическом ультразвуковом прозвучивании и акустическая активность. Главной целью опытов являлось выявление предвестников макроразрыва для установления стадии неустойчивости без знания внешней нагрузки и общей деформации модели. Было исследовано соотношение амплитуд фаз относительного сжатия и растяжения в последовательных циклах силовой вибрации, зарегистрированных датчиками напряжений, а также соотношение амплитуд последовательных фаз ультразвуковых импульсов и времен их вступления. Обнаружены эффект возникновения и развития асимметрии в первоначально синусоидальных циклах вибрации и искажение формы ультразвуковых сигналов при подходе модели к неустойчивости. Таким образом, экспериментально показана возможность определения стадии механической неустойчивости деформируемого тела по динамическим параметрам упругих колебаний во время последовательных знакопеременных фаз силового воздействия. Предполагается, что данный подход может быть реализован в натуральных условиях при изучении реакции геологической среды на земные приливы или сигналы искусственного вибропросвечивания.